

Electronic Supplementary Information

Enhancing electrochemical performance by triggering a local structure distortion in lithium vanadium phosphate cathode for lithium-ion batteries

Hyunyoung Park^{a,†}, Wontae Lee^{a,†}, Ranjth Thangavel^{a,d}, Woong Oh^a, Bong-Soo Jin^b, Won-Sub Yoon^{a,c,*}

^a Department of Energy Science, Sungkyunkwan University, 300 Suwon-si, Gyeonggi-do 440-746, Republic of Korea

^b Battery Research Center, Korea Electrotechnology Research Institute, Changwon 51543, Korea

^c SKKU Institute of Energy Science and Technology (SIEST), Sungkyunkwan University, Suwon 16419, Republic of Korea.

^dCurrent affiliation: School of Energy Science and Engineering, Indian Institute of Technology Guwahati, Guwahati 781039, India

*Corresponding author: wsubyoon@skku.edu

† These authors contributed to this work equally

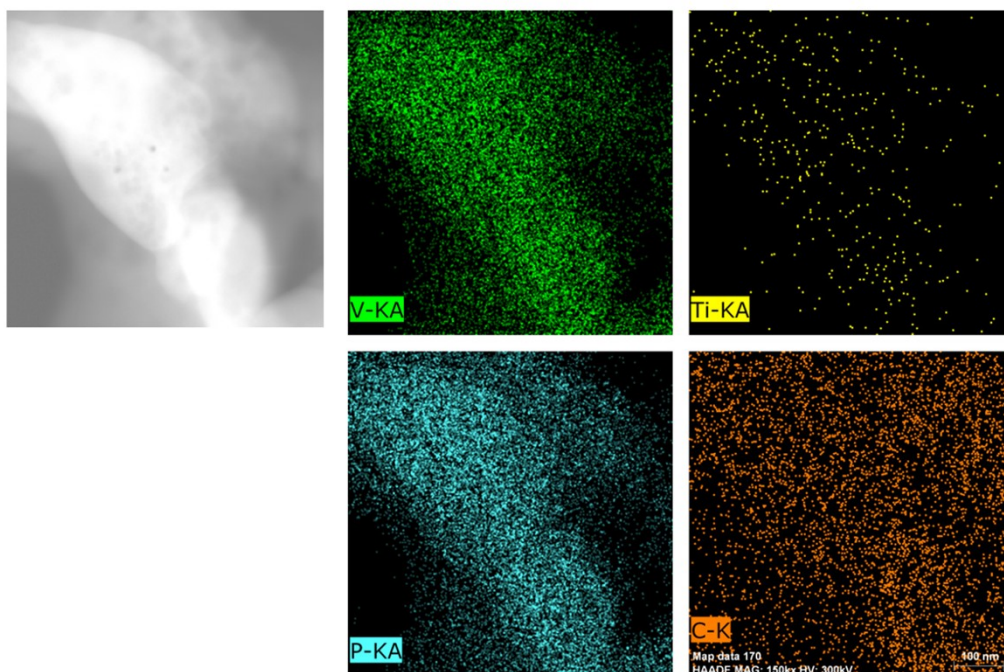


Figure S1. Energy-dispersive X-ray (EDX) mapping analysis of LVP-T particles from HRTEM

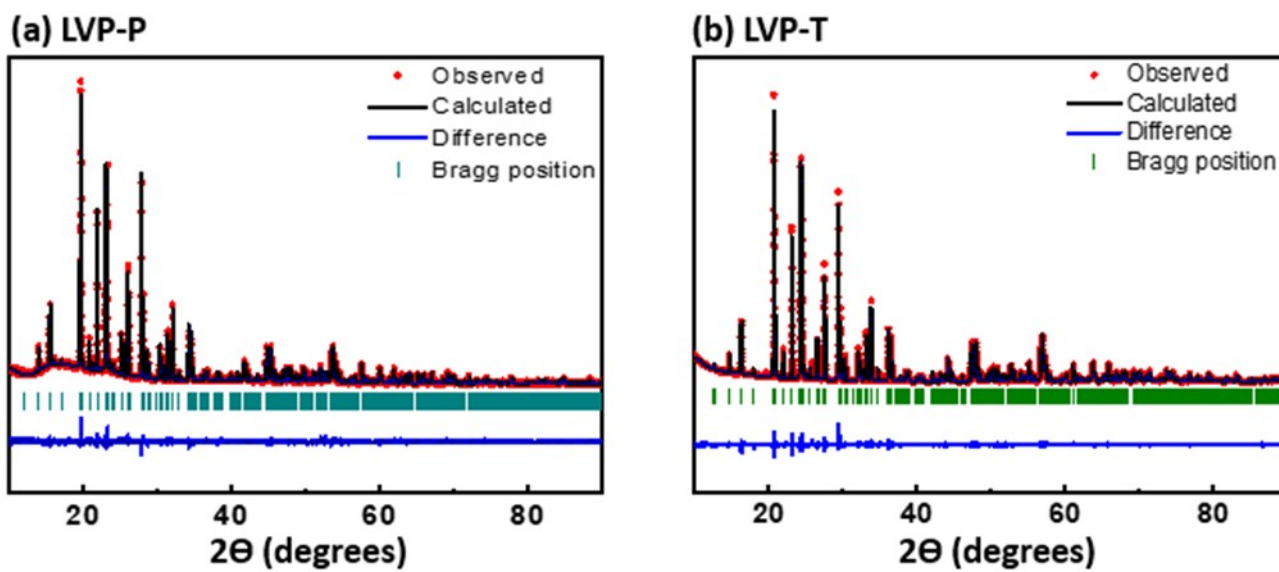


Figure S2. Observed and calculated pattern of (a) pristine LVP-P (reproduced from ref. 44 with permission from The Royal Society of Chemistry) and (b) pristine LVP-T of high-resolution powder diffraction

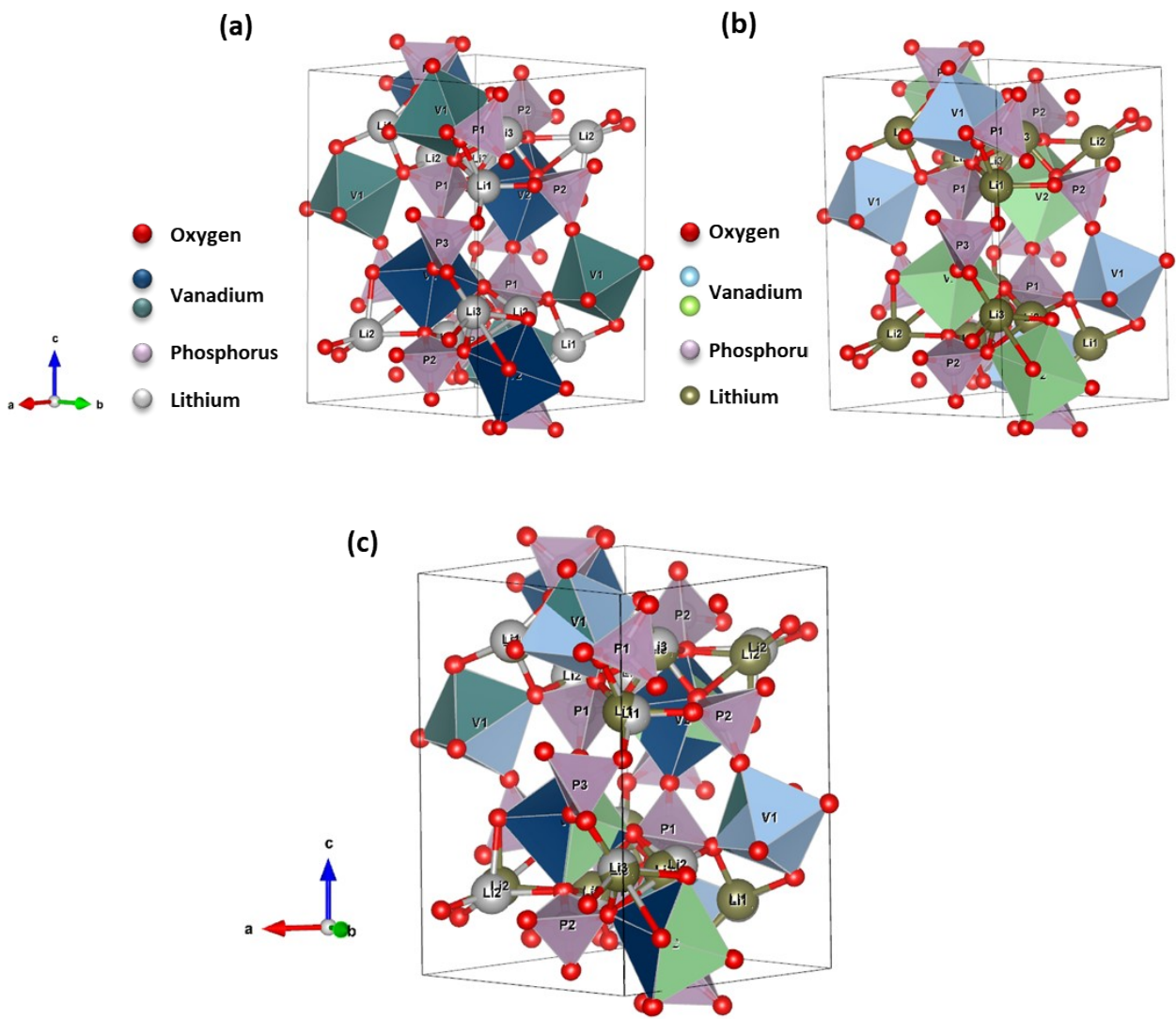
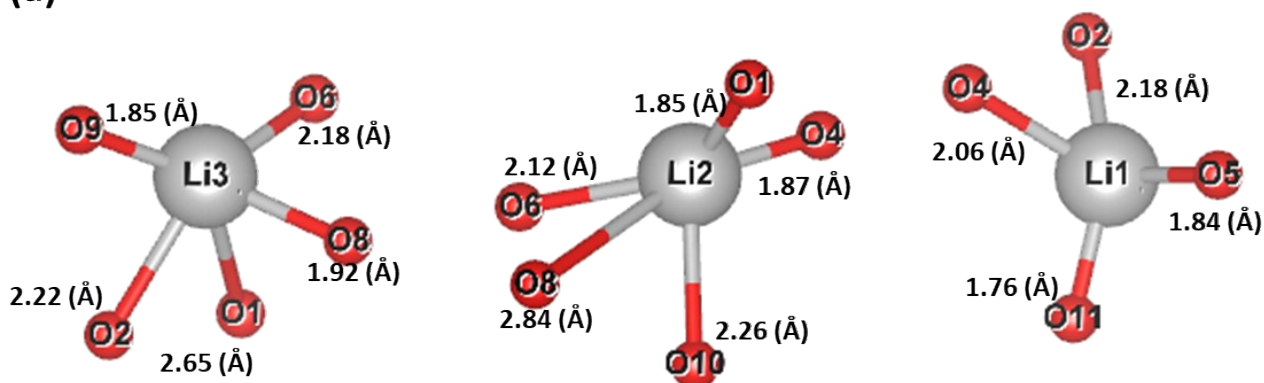


Figure S3. Crystal structures of (a) LVP-P, (b) LVP-T, and (c) overlapped crystal structures of both materials from Rietveld refinement of high-resolution powder diffraction.

(a)



(b)

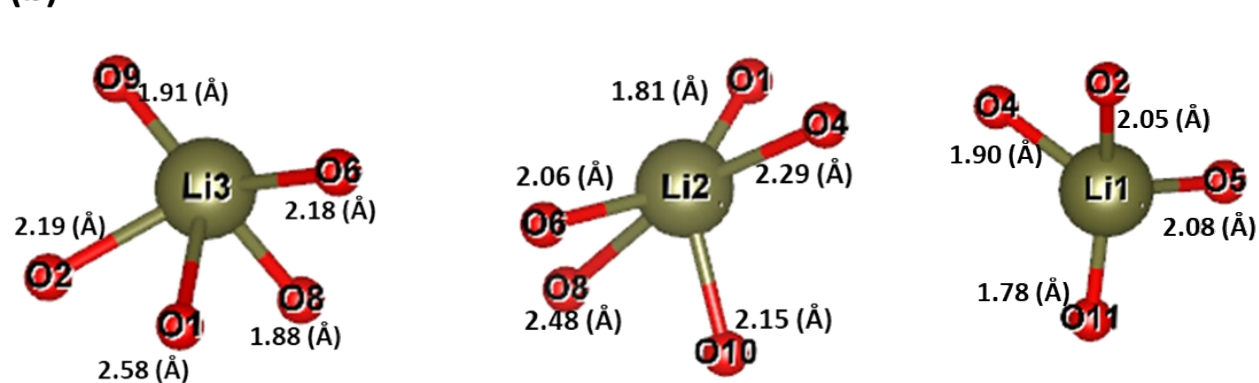


Figure S4. Each bond lengths around each three Li-ion site; (a) Li3 site, (b) Li2 site and (c) Li1 site in LVP-P and (d) Li3 site, (e) Li2 site, and (f) Li1 site in LVP-T in the crystal structures from Rietveld refinement of high-resolution powder diffraction.

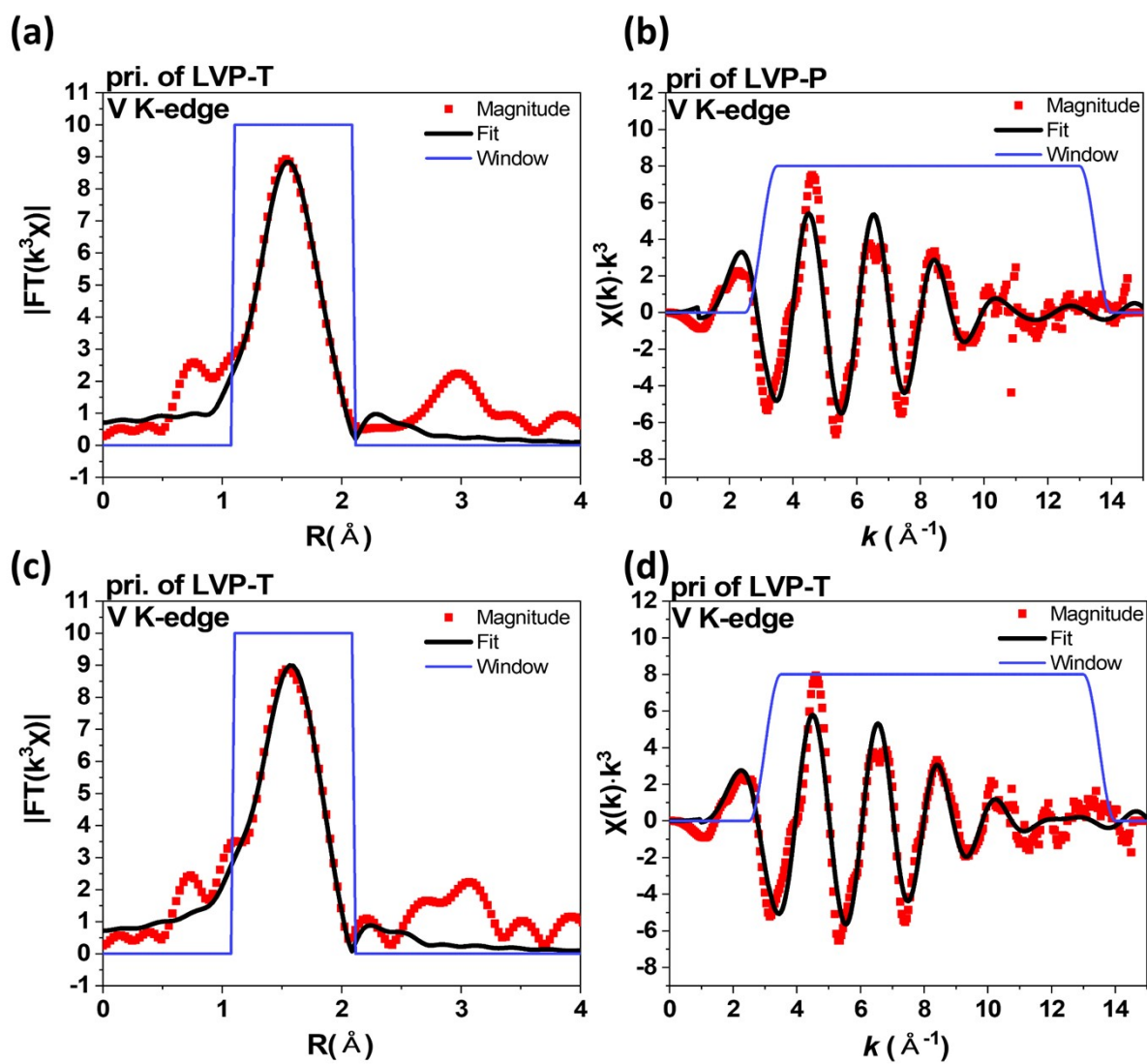


Figure S5. Nonlinear least-squares fitting on the EXAFS spectra of pristine LVP-P in (a) R-space and (b) k-space and pristine LVP-T in (c) R-space and (d) k-space. Both spectra are fitted simultaneously to obtain structural parameters listed in Table S5.

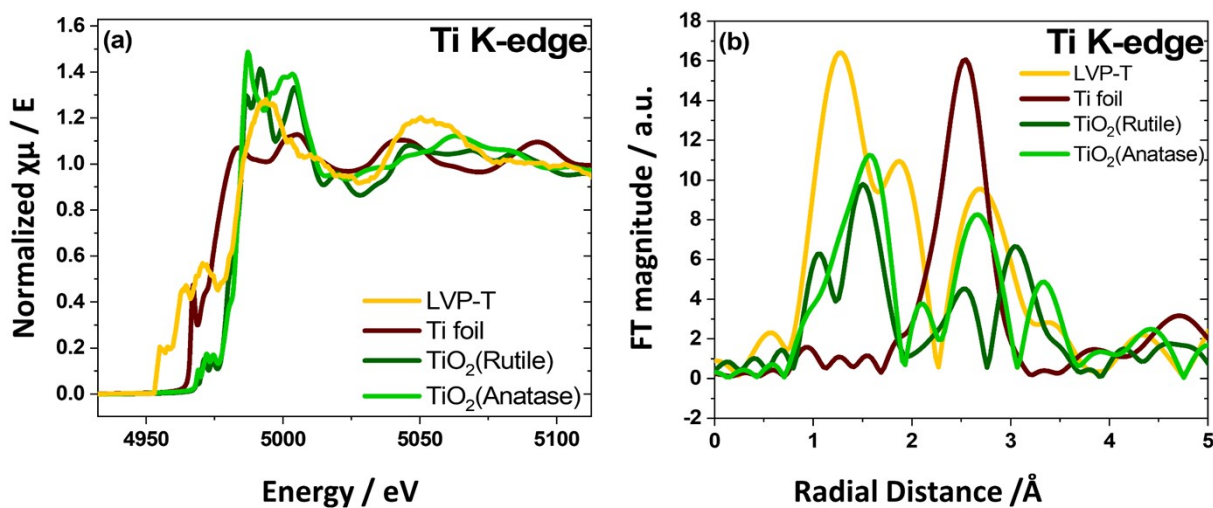


Figure S6. (a) Normalized XANES spectra and (b) magnified figure of XANES spectra at Ti K-edge at pristine LVP-T with references of Ti foil, TiO_2 (rutile), and $\text{TiO}_2(\text{anatase})$. (c) k^3 -weighted Fourier transformed EXAFS spectra at Ti K-edge at pristine state of LVP-T.

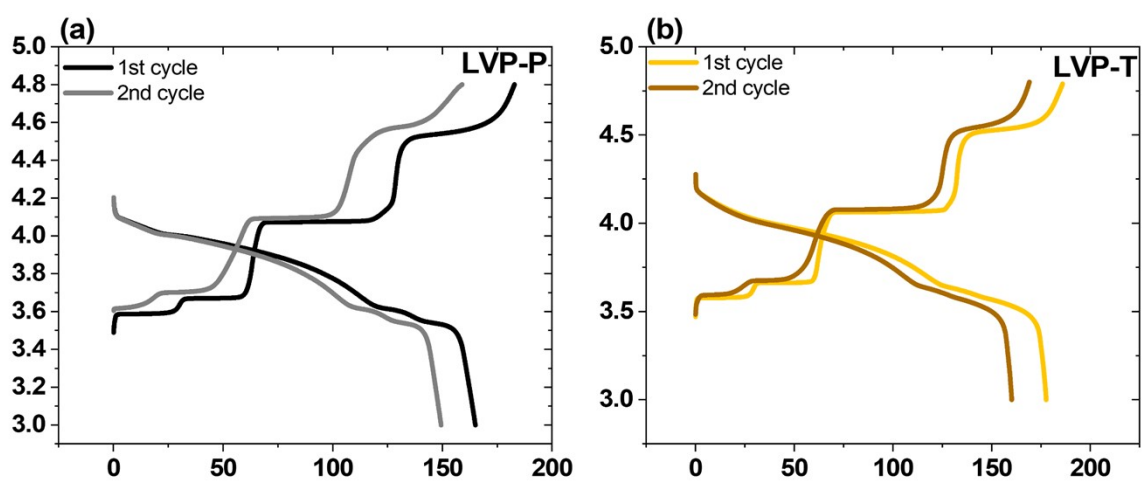
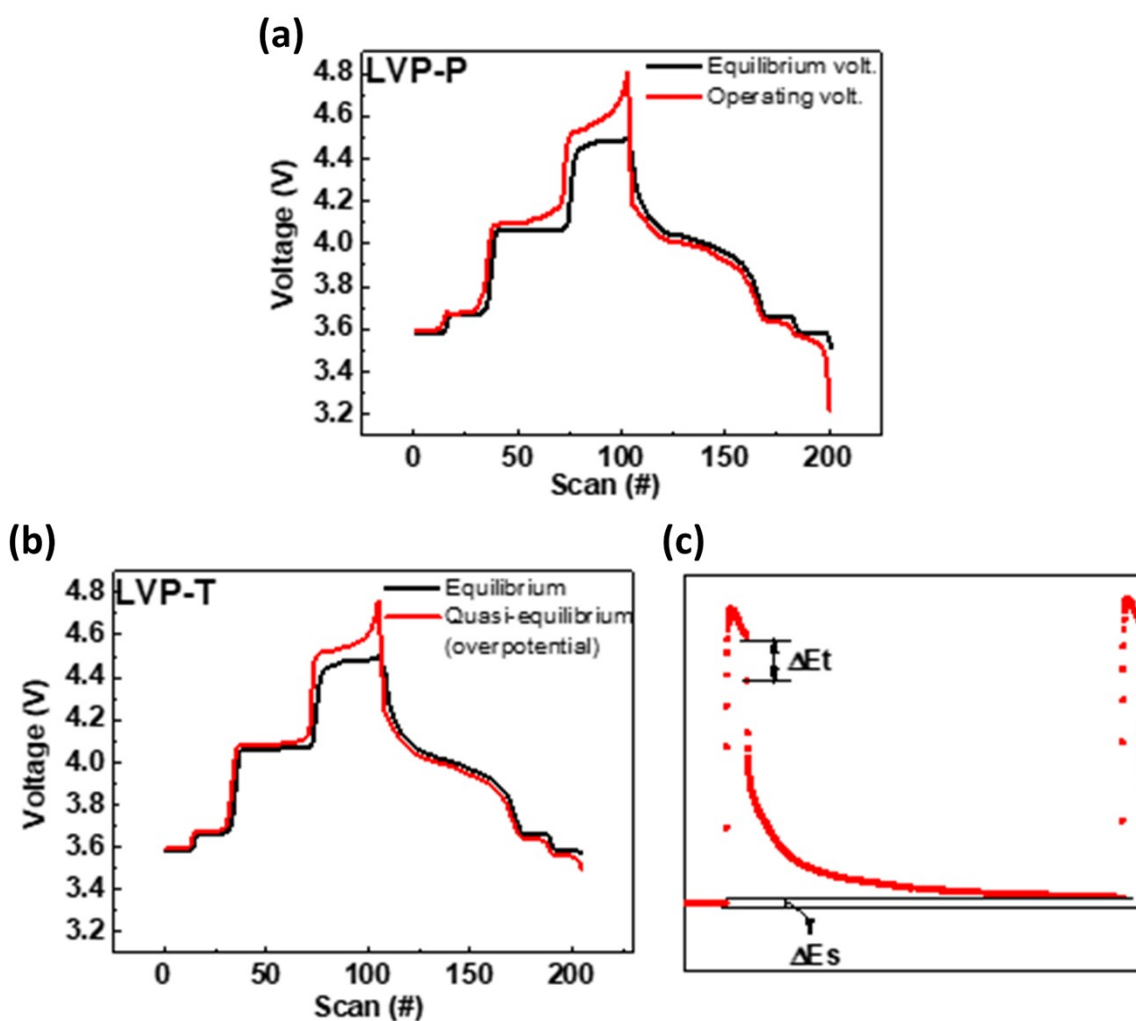


Figure S7. The electrochemical voltage profile of (a) LVP-P and (b) LVP-T during the initial two cycles at 0.1C



$$D_{Li^+} = \frac{4}{\pi\tau} \left(\frac{m_B V_M}{M_B A} \right)^2 \left(\frac{\Delta E_S}{\Delta E_T} \right)^2 \left(\tau \ll \frac{L^2}{D_{Li^+}} \right)$$

Figure S8. The equilibrium voltage (black) and operating voltage (red) in GITT test on (a) LVP-P (reproduced from ref. 44 with permission from The Royal Society of Chemistry) and (b) LVP-T during the first cycle and (c) magnified figure of LVP-T during the charge to be needed for calculating diffusion coefficient.

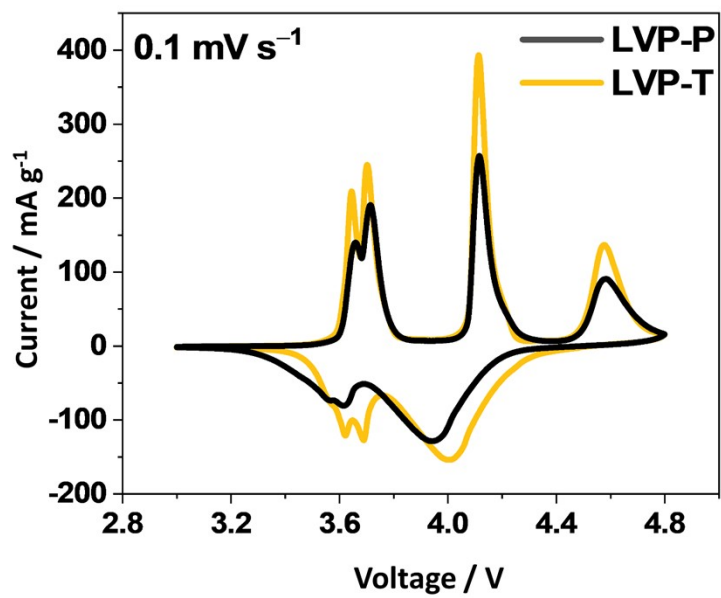


Figure S9. Cyclic voltammety curves of LVP-P and LVP-T electrodes

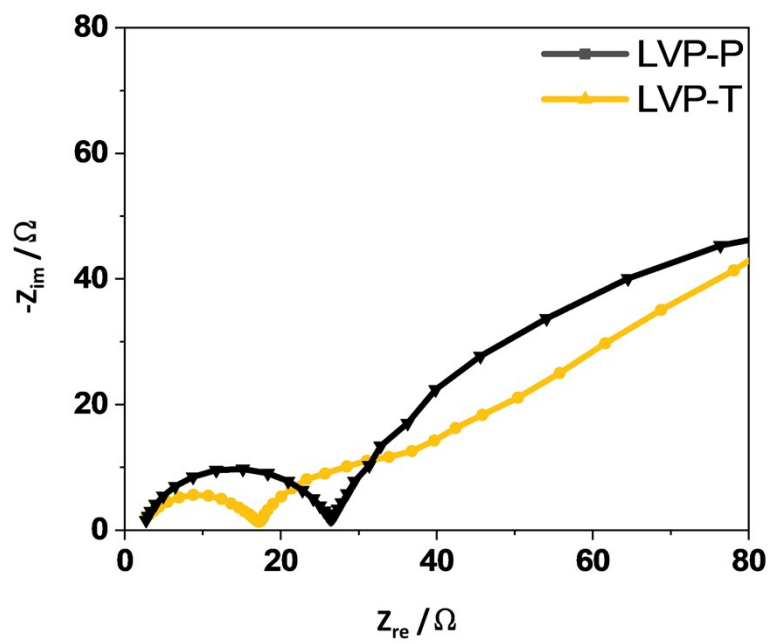


Figure S10. EIS spectra of LVP-P and LVP-T electrodes after the 1st charge/discharge cycle.

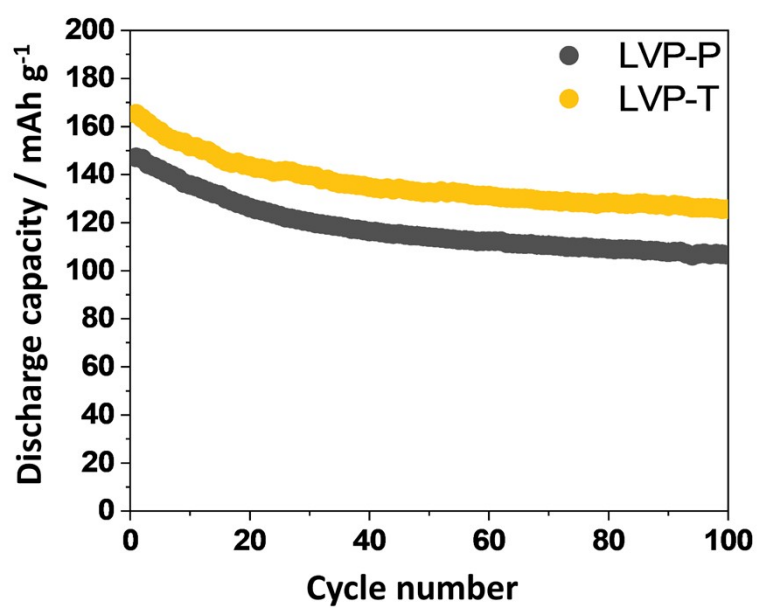


Figure S11. Cyclic stability test of LVP-P and LVP-T electrodes at 0.5C during 100 cycles

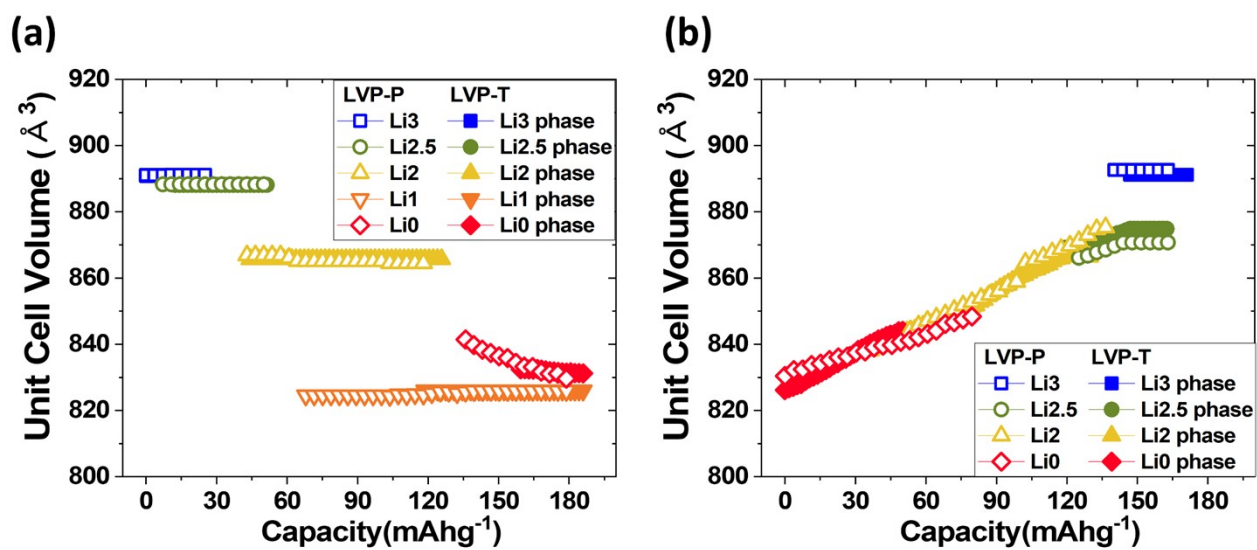


Figure S12. Change of unit cell volume obtained from in situ XRD patterns of LVP-P (unfilled, reproduced from ref. 44 with permission from The Royal Society of Chemistry) and LVP-T (filled) during (a) the 1st charge and (b) the 1st discharge

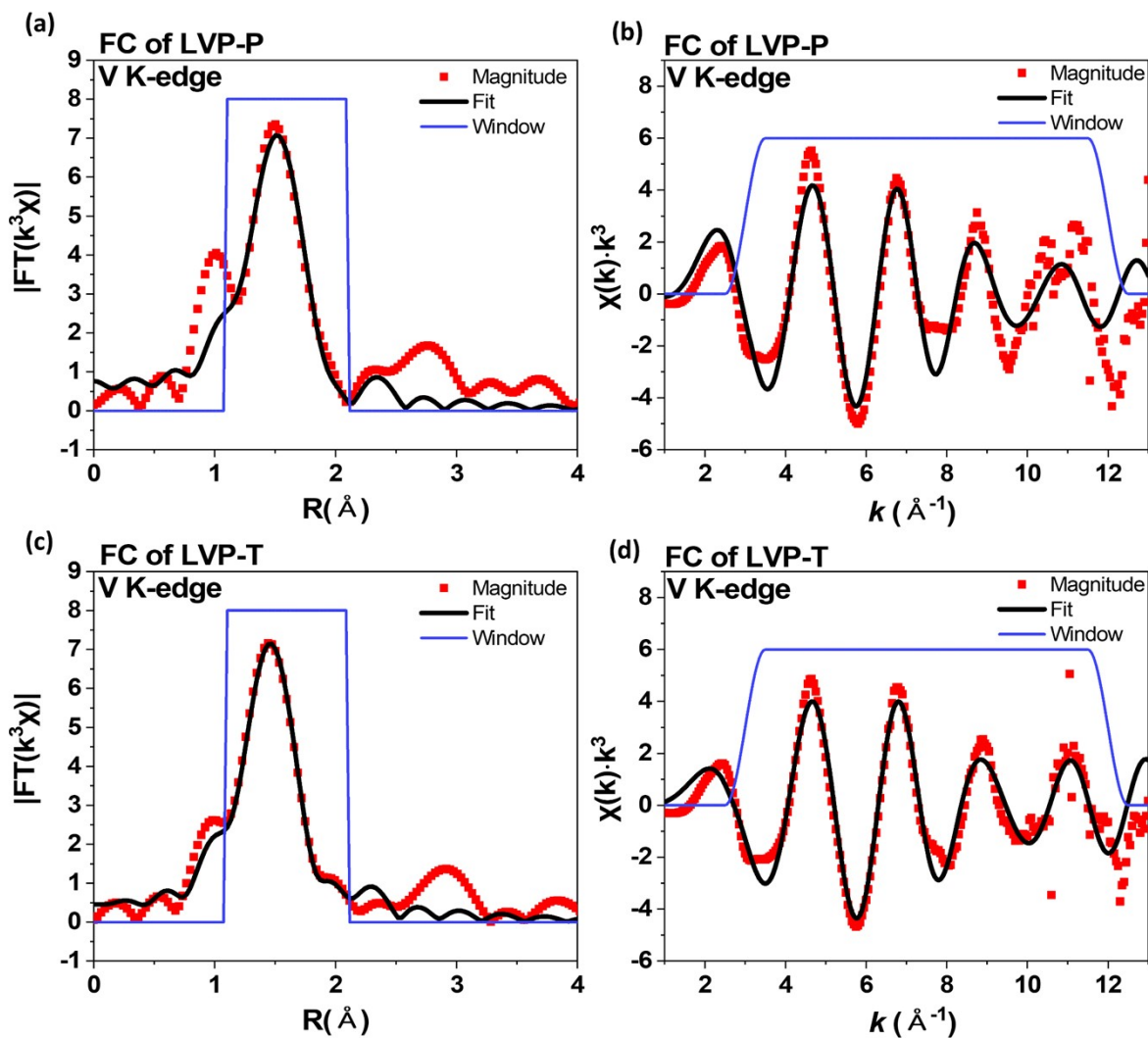


Figure S13. Nonlinear least-squares fitting on the EXAFS spectra of full charged LVP-P in R-space and k-space and full charged LVP-T in R-space and k-space. Both spectra are fitted simultaneously to obtain structural parameters listed in Table S6.

Table S1. Lattice parameters of LVP-P and LVP-T cathode materials obtained by Rietveld refinement of high-resolution powder diffraction

	a (Å)	b (Å)	c (Å)	Beta (°)	Vol. (Å³)
LVP-P	8.609(5)	8.594(5)	12.039(5)	90.593(5)	890.72(1)
LVP-T	8.609(1)	8.600(1)	12.041(1)	90.583(1)	891.42(1)

Table S2. Atomic position (x, y, z), temperature factors (B), and occupancy of each element obtained from the result of Rietveld refinement of pristine LVP-P and pristine LVP-T

*** : fixed**

For LVP-P, Rp= 5.36, Rwp= 7.11, Rexp= 5.12 and $\chi^2= 1.93$									
For LVP-T, Rp= 8.18 , Rwp= 11.5 , Rexp= 3.75 and $\chi^2= 3.28$									
Atom	x (Å)		y (Å)		z (Å)		B		Occ.
	LVP-P	LVP-T	LVP-P	LVP-T	LVP-P	LVP-T	LVP-P	LVP-T	
Li1	0.206(5)	0.227(3)	0.755(6)	0.772(4)	0.168(4)	0.175(4)	1*	1*	1*
Li2	0.955(6)	0.904(4)	0.303(5)	0.287(4)	0.216(4)	0.228(5)	1*	1*	1*
Li3	0.573(6)	0.572(2)	0.403(5)	0.405(2)	0.193(4)	0.199(6)	1*	1*	1*
V1	0.2470(8)	0.2476(3)	0.4619(7)	0.4630(5)	0.1113(5)	0.1106(4)	2.2(1)	0.8(6)	1*
V2	0.7519(8)	0.7522(2)	0.4707(7)	0.4706(4)	0.3897(5)	0.3902(3)	2.5(1)	0.9(6)	1*
P1	0.105(1)	0.106(1)	0.103(1)	0.104(2)	0.149(7)	0.149(8)	2.6(2)	1.8(3)	1*
P2	0.603(1)	0.604(1)	0.114(1)	0.115(4)	0.352(8)	0.352(3)	3.0(2)	1.1(8)	1*
P3	0.037(1)	0.035(5)	0.249(1)	0.249(7)	0.492(8)	0.492(1)	2.1(2)	1.4(5)	1*
O1	0.927(2)	0.928(1)	0.113(2)	0.112(9)	0.146(1)	0.144(1)	1.3(4)	0.2(3)	1*
O2	0.151(2)	0.154(9)	0.982(2)	0.980(6)	0.238(1)	0.236(6)	3.4(5)	0.9(5)	1*
O3	0.175(2)	0.176(7)	0.043(2)	0.042(1)	0.041(1)	0.041(7)	3.4(5)	0.8(3)	1*
O4	0.165(2)	0.163(2)	0.266(2)	0.266(9)	0.187(1)	0.185(2)	2.4(6)	1.2(3)	1*
O5	0.431(2)	0.434(6)	0.091(2)	0.091(7)	0.328(1)	0.328(6)	1.7(5)	0.2(8)	1*
O6	0.695(2)	0.697(3)	-0.002(2)	0.004(7)	0.279(1)	0.278(2)	2.7(6)	0.2(8)	1*
O7	0.650(2)	0.650(8)	0.083(2)	0.084(6)	0.470(1)	0.469(6)	4.8(6)	1.3(8)	1*
O8	0.642(2)	0.645(1)	0.283(2)	0.281(1)	0.318(1)	0.317(6)	2.4(5)	1.3(4)	1*
O9	0.951(2)	0.953(4)	0.133(2)	0.133(8)	0.568(1)	0.567(7)	1.8(4)	1.1(6)	1*
O10	0.935(2)	0.934(6)	0.318(2)	0.319(5)	0.403(1)	0.404(1)	3.1(6)	0.2(1)	1*
O11	0.171(2)	0.171(1)	0.174(2)	0.174(5)	0.432(1)	0.432(9)	2.3(5)	1.3(5)	1*
O12	0.109(2)	0.112(3)	0.362(2)	0.355(3)	0.573(1)	0.573(5)	2.2(5)	1.4(7)	1*

Table S3. O-O distance surrounding Li-ion sites in pristine LVP-P and pristine LVP-T in the crystal structures obtained from Rietveld refinement of high-resolution powder diffraction

	LVP-P (Å)		LVP-T (Å)		Difference (Å)
Li1	O2-O4	2.60 (9)	O2-O4	2.58 (8)	-0.02
	O2-O5	3.52 (11)	O2-O5	3.52 (9)	0
	O2-O11	3.69 (7)	O2-O11	3.67 (9)	-0.02
	O4-O5	3.21 (8)	O4-O5	3.24 (8)	0.03
	O4-O11	3.05 (10)	O4-O11	3.05 (11)	0
	O5-O11	2.67 (6)	O5-O11	2.69 (8)	0.02
	Volume	3.14	Volume	3.15	0.01
Li2	O1-O4	2.48 (8)	O1-O4	2.46 (5)	-0.02
	O1-O6	3.59 (10)	O1-O6	3.66 (6)	0.07
	O1-O8	3.54 (3)	O1-O8	3.52 (5)	-0.02
	O1-O10	3.56 (7)	O1-O10	3.58 (3)	0.02
	O4-O6	3.71 (6)	O4-O6	3.74 (6)	0.03
	O4-O8	4.79 (18)	O4-O8	4.74 (4)	-0.05
	O4-O10	3.32 (6)	O4-O10	3.32 (5)	0
	O6-O8	2.60 (3)	O6-O8	2.62 (6)	0.02
	O6-O10	2.90 (6)	O6-O10	2.92 (5)	0.02
	O8-O10	2.73 (5)	O8-O10	2.71 (6)	-0.02
	Volume	6.95	Volume	7.03	0.08
Li3	O1-O2	2.48 (1)	O1-O2	2.50 (5)	0.02
	O1-O6	2.76 (3)	O1-O6	2.72 (4)	-0.04
	O1-O8	2.93(3)	O1-O8	2.95 (1)	0.02
	O1-O9	4.17 (4)	O1-O9	4.17 (8)	0
	O2-O6	3.96 (7)	O2-O6	3.97 (3)	0.01
	O2-O8	3.12 (3)	O2-O8	3.15 (5)	0.03
	O2-O9	2.69 (18)	O2-O9	2.71 (11)	0.02
	O6-O8	2.60 (3)	O6-O8	2.62 (6)	0.02
	O6-O9	3.72 (4)	O6-O9	3.72 (6)	0
	O8-O9	3.49 (3)	O8-O9	3.50 (10)	0.01
	Volume	6.19	Volume	6.28	0.09

Table S4. O-Li-O angles surrounding Li-ion sites in pristine LVP-P and pristine LVP-T in the crystal structures obtained from Rietveld refinement of high-resolution powder diffraction

	LVP-P (°)		LVP-T (°)	
Li1	O11-Li1-O4	106.1	O11-Li1-O4	112.3
	O11-Li1-O2	138.6	O11-Li1-O2	147.2
	O11-Li1-O5	96.2	O11-Li1-O5	88.5
	O4-Li1-O2	75.2	O4-Li1-O2	81.3
	O4-Li1-O5	111.5	O4-Li1-O5	109.4
	O2-Li1-O5	122.3	O2-Li1-O5	117.1
Li2	O1-Li2-O8	91.3	O1-Li2-O8	109.0
	O1-Li2-O6	129.4	O1-Li2-O6	142.3
	O1-Li2-O10	119.4	O1-Li2-O10	129.2
	O1-Li2-O4	84.0	O1-Li2-O4	73.1
	O8-Li2-O6	58.6	O8-Li2-O6	70.1
	O8-Li2-O10	61.0	O8-Li2-O10	71.1
	O8-Li2-O4	161.7	O8-Li2-O4	166.3
	O6-Li2-O10	83.3	O6-Li2-O10	88.3
	O6-Li2-O4	137.4	O6-Li2-O4	118.2
	O10-Li2-O4	106.7	O10-Li2-O4	97.3
Li3	O9-Li3-O6	134.7	O9-Li3-O6	131.3
	O6-Li3-O8	79.4	O6-Li3-O8	80.3
	O8-Li3-O1	78.1	O8-Li3-O1	81.3
	O1-Li3-O2	60.6	O1-Li3-O2	63.3
	O2-Li3-O9	82.1	O2-Li3-O9	82.3
	O6-Li3-O1	68.8	O6-Li3-O1	69.3
	O9-Li3-O1	135.4	O9-Li3-O1	136.3
	O9-Li3-O8	136.3	O9-Li3-O8	135.3
	O2-Li3-O6	129.4	O2-Li3-O6	131.5
	O2-Li3-O8	98.3	O2-Li3-O8	101.3

Table S5. Structural parameters derived from the EXAFS fitting for pristine LVP-P and pristine LVP-T. Amplitude reduction factors ($S0^2$) for the V K-edge spectra are fixed as 0.7. R, σ^2 , and ΔE denote interatomic distance, degree of disorder, and inner potential shift parameter, respectively.

For LVP-P, the reliable factors are $\chi^2 = 32.11$, and R-factor = 0.0073.

For LVP-T, the reliable factors are $\chi^2 = 37.48$, and R-factor = 0.0029.

The structural model of $\text{Li}_3\text{V}_2(\text{PO}_4)_3$ in Yin et al. was used for fitting V-O coordination.

Fit (R=1.2 Å – 2.1 Å) (k=3 Å ⁻¹ - 13.5 Å ⁻¹) (S0 ² =0.7)		Pristine of LVP-P ($\Delta E = -0.4 \pm 0.7$)		Pristine of LVP-T ($\Delta E = 2.2 \pm 0.5$)		Debye-Waller factor (σ^2)
Coordination number (V-O)		R(Å)	σ^2	R(Å)	σ^2	Difference (LVP-T)-(LVP-P)
V1-O7	1	1.76 ± 0.07	0.005 ± 0.007	1.74 ± 0.04	0.010 ± 0.004	0.005
V1-O11	2	1.930 ± 0.005	0.0003 ± 0.0005	1.926 ± 0.005	0.0009 ± 0.0004	0.0006
V1-O2	1	2.05 ± 0.02	0.002 ± 0.002	2.05 ± 0.03	0.0043 ± 0.0006	0.002
V1-O5	1	2.06 ± 0.01	0.0006 ± 0.0013	2.07 ± 0.04	0.001 ± 0.005	0.0011
V1-O4	1	2.11 ± 0.02	0.003 ± 0.002	2.12 ± 0.01	0.003 ± 0.001	0
V2-O12	2	1.89 ± 0.01	0.003 ± 0.001	1.90 ± 0.01	0.005 ± 0.001	0.002
V2-O1	3	2.01 ± 0.02	0.003 ± 0.001	2.026 ± 0.008	0.002 ± 0.0006	-0.001
V2-O6	1	2.39 ± 0.02	0.002 ± 0.003	2.38 ± 0.01	0.002 ± 0.002	0

Table S6. Structural parameters derived from the EXAFS fitting for the full charged states (FC) of LVP-P and LVP-T. Amplitude reduction factors (S_0^2) for the V K-edge spectra are fixed as 0.7. R, σ^2 , and ΔE denote interatomic distance, degree of disorder, and inner potential shift parameter, respectively.

For LVP-P, the reliable factors are $\chi^2 = 13.35$, and R-factor = 0.0064.

For LVP-T, the reliable factors are $\chi^2 = 17.36$, and R-factor = 0.0098.

The structural model of $\text{Li}_3\text{V}_2(\text{PO}_4)_3$ in Yin et al. was used for fitting V-O coordination.

Fit ($R=1.2 \text{ \AA} - 2.1 \text{ \AA}$) ($k=3 \text{ \AA}^{-1} - 13.5 \text{ \AA}^{-1}$) ($S_0^2=0.7$)		FC of LVP-P ($\Delta E_0 = 5.7 \pm 0.9$)		FC of LVP-T ($\Delta E_0 = 4.1 \pm 1.0$)		Debye-Waller factor (σ^2)
Coordination number (V-O)		R(\AA)	σ^2	R(\AA)	σ^2	Difference (LVP-T)-(LVP-P)
V1-O7	1	1.63 \pm 0.02	0.005 \pm 0.003	1.59 \pm 0.02	0.006 \pm 0.003	0.001
V1-O11	2	1.862 \pm 0.005	0.0031 \pm 0.0005	1.845 \pm 0.009	0.0036 \pm 0.0001	0.0006
V1-O2	1	1.889 \pm 0.02	0.001 \pm 0.002	1.887 \pm 0.013	0.001 \pm 0.001	0.000
V1-O5	1	2.06 \pm 0.02	0.004 \pm 0.003	2.05 \pm 0.04	0.007 \pm 0.005	0.003
V1-O4	1	2.23 \pm 0.02	0.002 \pm 0.002	2.23 \pm 0.01	0.003 \pm 0.001	0.001
V2-O12	2	1.98 \pm 0.02	0.001 \pm 0.002	1.94 \pm 0.01	0.0023 \pm 0.0008	0.0013
V2-O1	3	2.05 \pm 0.01	0.008 \pm 0.002	2.05 \pm 0.04	0.005 \pm 0.001	-0.003
V2-O6	1	2.39 \pm 0.02	0.0003 \pm 0.002	2.37 \pm 0.03	0.0022 \pm 0.0039	0.0019